ISSN 1070-3632, Russian Journal of General Chemistry, 2013, Vol. 83, No. 12, pp. 2488–2501. © Pleiades Publishing, Ltd., 2013.

Complexes of Nalidixic Acid with Some Vital Metal Ions: Synthesis, Chemical Structure Elucidation, and Antimicrobial Evaluation[1]

M. Zaky[a], Mohamed Y. El-Sayed[a,b], Samy M. El-Megharbel[a,c], Sameh Abo Taleb[a], and Moamen S. Refat[c,d]

[a] *Department of Chemistry, Faculty of Science, Zagazig University, Egypt*
[b] *Faculty of Applied Medical Science, Al Jouf University-Al Qurayate*
[c] *Department of Chemistry, Faculty of Science, Taif University, 888 Taif, Kingdom Saudi Arabia*
[d] *Department of Chemistry, Faculty of Science, Port Said, Port Said University, Egypt*
e-mail: msrefat@yahoo.com

Received October 7, 2013

Abstract—Complexes of nalidixic acid with Ca(II), Mg(II), Zn(II), Fe(III), and VO(II) ions, have been synthesized and characterized by means of microanalysis, conductance, IR, NMR and UV-Vis spectroscopy and thermogravimetric (TGA/DTG and DTA) measurements. The ligand coordinates in a bidentate mode via one carboxylate oxygen atom and the oxygen atom of the pyridine carbonyl group. The kinetic thermodynamic parameters such as: activation energy E^*, ΔH^*, ΔS^*, and ΔG^* have been estimated using Coats and Redfern as well as Horowitz–Metzger equations. Antimicrobial activity of the obtained complexes against some kinds of bacteria and fungi has been evaluated.

DOI: 10.1134/S1070363213120475

INTRODUCTION

Study of the interaction between drugs and metal ions is an important and active research area in bioinorganic chemistry [1–4]. It is well known that the action of many drugs is dependent on the coordination with metal ions [1] or the inhibition [2] on the formation of metalloenzymes. Quinolones is a class of antibacterial agents, known for over 40 years [5]. Presence of metal ions considerably alters the activity of quinolones against potentially susceptible bacteria [6]. The interaction of metal ions with diverse deprotonated quinolones as ligands has been thoroughly discussed [7–16]. Quinolones have been classified in generations based on their activity [17]. Each generation represents an enhanced spectrum of activity in comparison to a previous one. Nalidixic acid (Fig. 1) is an example of first-generation quinolones that are active against Gram-negative organisms and they are used for the treatment of uncomplicated urinary tract infections [18]. The association complexes between nalidixic acid and different metal ions has been described [19–25]. Copper(II) and calcium complexes have been studied in [19]. Nakano et al. [22] studied the corresponding complexes of nalidixic acid with Al^{3+}, Mg^{2+} and Ca^{2+} ions.

In this work, the coordination mode of nalidixic acid chelating metal ions such as Ca(II), Mg(II), Zn(II), Fe(III), and VO(II) have been investigated. The antibacterial and antifungal activities of the prepared complexes also were evaluated.

EXPERIMENTAL

All chemicals used in this investigation were of analytical grade and used without further purification (Merck). $CaCl_2$, $MgCl_2 \cdot 6H_2O$, $ZnSO_4 \cdot H_2O$, $Fe(NO_3)_3 \cdot 9H_2O$, and $VOSO_4 \cdot H_2O$ were used to prepare corresponding target complexes. Nalidixic acid was received from Egyptian International Pharmaceutical Industrial Company (EIPICO). Carbon, hydrogen and

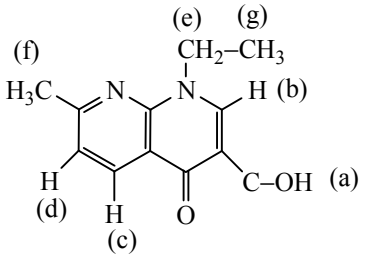

Fig. 1. Nalidixic acid (Ndx).

[1] The text was submitted by the authors in English.

Table 1. Elemental analysis and physical data of nalidixic acid complexes

Complex	M_W, g/mol	mp, °C	Color	C, %	H, %	N, %	M, %	Λ, Ω^{-1} cm^2 mol^{-1}
				calculated/ found	calculated/ found	calculated/ found	calculated/ found	
I	359.5	> 260	White	40.05/40.72	5.01/5.12	11.68/11.70	11.12/10.87	20
II	703.5	> 260	White	20.46/20.94	8.24/7.65	5.97/6.10	3.41/3.29	33
III	482.4	> 260	Eellowish white	29.85/29.94	4.77/4.70	8.71/8.54	13.55/13.31	6
IV	481.0	> 260	Pale brown	29.93/29.54	4.36/4.53	17.46/17.58	11.64/11.37	36
V	448.0	> 260	Green	32.14/31.67	4.24/5.05	9.37/9.56	14.95/14.87	7

nitrogen content were determined using a Perkin-Elmer CHN Elemental Analyzer model 2400. The metal content was found gravimetrically by converting the compounds into their corresponding oxides. Molar conductivities of freshly prepared 1.0×10^{-3} mol/L DMSO solutions of the complexes were measured using Jenway 4010 conductivity meter. IR spectra were recorded on a Bruker FTIR spectrophotometer (4000–400 cm^{-1}) in KBr pellets. UV-Vis spectra were recorded using Jenway 6405 spectrophotometer with 1 cm quartz cell, in the 200–600 nm range(DMSO as solvent, 1.0×10^{-3} M complex concentration). ^{1}H NMR spectra were recorded on a Varian Gemini 200 MHZ machine using DMSO-d_6 as solvent and TMS as internal reference. Thermogravimetric analysis (TGA, DTG and DTA) were carried out in the temperature range from 25 to 800°C in nitrogen atmosphere using Shimadzu TGA-50 H thermal analyzer(platinum crucible, nitrogen atmosphere with a 30 mL/min flow rate and a heating rate of 10°C/min).

Preparation of the complexes. For all preparations, doubly distilled water was used as a solvent. Nalidixic acid complexes: [Ca(Ndx)(Cl)(NH$_3$)(H$_2$O)$_2$] (**I**), [Mg(Ndx)(Cl)(NH$_3$)(H$_2$O)$_2$]·20H$_2$O (**II**), [Zn(Ndx)·(SO$_4$)(NH$_4$)(H$_2$O)]·3H$_2$O (**III**), [Fe(Ndx)(NO$_3$)$_2$(NH$_3$)$_2$]·2H$_2$O (**IV**) and [VO(Ndx)(SO$_4$)(NH$_4$)]·2H$_2$O (**V**) were prepared, using a 1 : 1 (metal : Ndx) ratio. The complexes were prepared by mixing equal volumes (20 mL) of distilled water solution of CaCl$_2$ (0.111 g, 1.0 mmol), MgCl$_2$·6H$_2$O (0.203 g, 1.0 mmol), ZnSO$_4$·H$_2$O (0.180 g, 1.0 mmol), Fe(NO$_3$)$_3$·9H$_2$O (0.404 g, 1.0 mmol) and VOSO$_4$·H$_2$O (0.163 g, 1.0 mmol), respectively with a solution of nalidixic acid (0.232 g, 1.0 mmol) in 20 mL of methanol. The mixtures were neutralized with 5% alcoholic ammonia solution to pH 7.0–9.0, then warmed at about ~60°C for about 45 min and left to evaporate slowly at room temperature overnight. The obtained precipitates were filtered off, washed several times with minimum amount of hot methanol and dried at 60°C over anhydrous CaCl$_2$. Colored solid complexes were obtained in moderate to good yields (65–70%). The physical and analytical data, colors, elemental analysis data (CHN, Me) and melting/decomposition temperatures of the compounds are presented in Table 1. The found and calculated CHN contents are in a well agreement with each other and prove the suggested molecular formula of the resulted complexes. The complexes have high melting points above > 260°C. They are air-stable, insoluble in water, partially soluble in alcohol and most of organic solvents. Soluble in DMSO, DMF and concentrated acids. The nalidixic acid ligand behaves as bidentate ligand and coordinates to the metal ions via one carboxylate oxygen atom and the oxygen atom of the pyridine carbonyl group.

RESULTS AND DISSCUSSION

In recent years there has been increasing interest in determining the rate-dependent parameters of solid-state non-isothermal decomposition reactions by analysis of TG curves [26–32]. Most commonly used methods are the differential method of Freeman and Carroll [26] integral method of Coat and Redfern [27] and the approximation method of Horowitz and Metzger [30].

In the present investigation, the general thermal behavior of the nalidixic acid metal complexes in terms of stability ranges, peak temperatures and values of kinetic parameters are discussed. The kinetic parameters have been evaluated using the Coats-Redfern equation:

$$\int_{\alpha}^{0} \frac{d\alpha}{(1-\alpha)^n} = \frac{A}{\varphi}\int_{T_1}^{T_2} \exp\left[-(E^*/RT)\right]dt. \qquad (1)$$

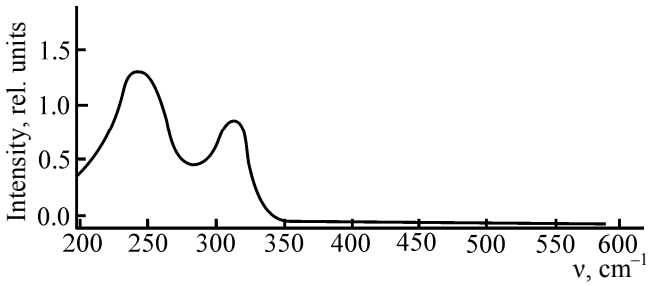

Fig. 2. UV-Vis electronic spectra of Zn(II) complex **III**.

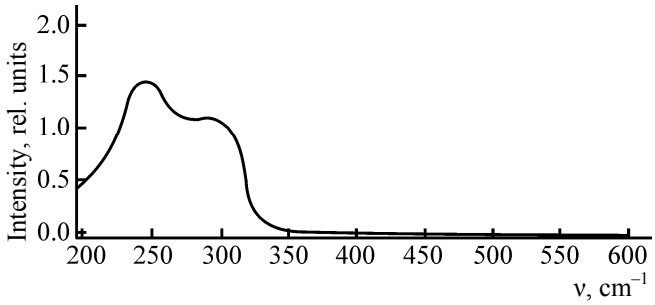

Fig. 3. UV-Vis electronic spectra of VO(II) complex **V**.

This equation on integration gives

$$\ln\left[-\frac{\ln(1-\alpha)}{T^2}\right] = -\frac{E^*}{RT} + \ln\left[\frac{AR}{\varphi E^*}\right]. \quad (2)$$

A plot of left-hand side (LHS) against $1/T$ was drawn. E^* is the energy of activation in J mol^{-1} and calculated from the slop and A in (s^{-1}) from the intercept value. The entropy of activation ΔS^* in (J K^{-1} mol^{-1}) was calculated by using the equation:

$$\Delta S^* = R\ln(Ah/k_B T_s), \quad (3)$$

where k_B is the Boltzmann constant, h is the Plank's constant and T_s is the DTG peak temperature [33].

The Horowitz–Metzger equation is an illustrative of the approximation methods.

$$\log[\{1-(1-\alpha)^{1-n}\}/(1-n)] = E^*\theta/2.303RT_s^2,\ n \neq 1. \quad (4)$$

When n = 1, the LHS of Eq. (4) would be log [–log (1 – α)]. For a first-order kinetic process the Horowitz–Metzger equation may be written in the form:

$$\log[\log(w_\alpha/w_\gamma)] = E^*\theta/2.303RT_s^2 - \log 2.303,$$

where $\theta = T - T_s$, $w_\gamma = w_\alpha - w$, w_α = mass loss at the completion of the reaction; w = mass loss up to time t. The plot of log [log (w_α /w_γ)] vs θ was drawn and found to be linear from the slope of which E^* was calculated. The pre-exponential factor, A, was calculated from the equation:

$$E^*/RT_s^2 = A/[\varphi\exp(-E^*/RT_s)].$$

The entropy of activation, ΔS^*, was calculated from Eq. (3). The enthalpy activation, ΔH^*, and Gibbs free energy, ΔG^*, were calculated from; $\Delta H^* = E^* - RT$ and $\Delta G^* = \Delta H^* - T\Delta S^*$, respectively.

Molar conductivity. Conductivity measurements have frequently been used to predicts the structure of metal chelates within limits of their solubility. They provide a method of testing the degree of ionization of the complexes. The more ions complex liberates in solution, the higher will be its molar conductivity and vice versa [35]. The molar conductivity values for the Ca(II), Mg(II), Zn(II), Fe(III), and VO(II) complexes of nalidixic acid in DMSO solvent (1.00×10^{-3} M) were found to be in the range 6–36 Ω^{-1} cm^2 mol^{-1} at 25°C, suggesting them to be non-electrolytes [36] as shown in Table 1. Hence the molar conductance values indicate that no ions are present outside the coordination sphere so Cl^- , SO_4^{2-} and NO_3^- ions may exist inside the coordination sphere or absent. The obtained results were strongly matched with the elemental analysis data where Cl^-, and SO_4^{2-} ions were detected in case of Ca(II), Mg(II), Zn(II), Fe(III), and VO(II) complexes after decomposition of these complexes with nitric acid followed by addition of $AgNO_3$ and $BaCl_2$ solutions respectively. NO_3^- ions were detected using infrared spectral data.

Electronic absorption spectra of nalidixic acid complexes. The formation of the Ca(II), Mg(II), Zn(II), VO(II), and Fe(III) complexes with nalidixic acid were also confirmed by UV-Vis spectra. Figures 2 and 3 show the electronic absorption spectra of the Zn(II) and VO(II) complexes in DMSO in the 200–600 nm range. It is known that the free nalidixic acid has two distinct absorption bands at 254 and 356 nm which assigned to π→π* and n→π* transitions respectively [37]. These transitions occur in case of unsaturated hydrocarbons, which contain carbon atom connected with oxygen atoms as in carboxylic and ketone groups [38]. These two bands of free nalidixic acid are clearly hypsochromically affected (blue shifted) in the electronic spectra of Zn(II) and VO(II) complexes which show two absorption bands at 244 and 325 nm for Zn(II) complex and at 248 and 304 nm for VO(II) complex assigned to π→π* and n→π*

Table 2. IR frequencies (cm^{-1}) of nalidixic acid and its metal complexes

Compound	ν(O–H); COOH and H_2O	ν(N–H); NH_3 and NH_4	δ(N–H); NH_3 and NH_4	ν(C=O); COOH	ν(C=O); Ketonic	$\nu_{as}(COO^-)$	$\nu_s(COO^-)$	Δν	ν(C–O)	ν(M–O)	ν(M–N)
Nalidixic acid	3410	–	–	1717	1618	–	–	–	1229	–	–
I	3430	3164	1442	–	1621	1573	1353	220	1257	546	451
II	3407	3150	1445	–	1640	1577	1358	219	1259	622	487
III	3400	3240	1442	–	1623	1570	1353	217	1258	500	435
IV	3430	3145	1441	–	1620	1564	1360	204	1257	512	444
V	3462	3200	1446	–	1628	1562	1360	202	1284	539	450

transitions respectively. This hypsochromically change in the spectra of Zn(II) and VO(II) complexes indicate that the carboxylic group and ketone groups are involved in the complexation. These results are clearly in accordance with the results of FT-IR and ^1H NMR spectra.

Infrared spectra of nalidixic acid complexes. The infrared spectra of nalidixic acid and its complexes under investigation are shown in Figs. 4–8 and Table 2. The spectra are similar but there are some differences which could give indication on the type of coordination. The infrared spectra of the free nalidixic acid

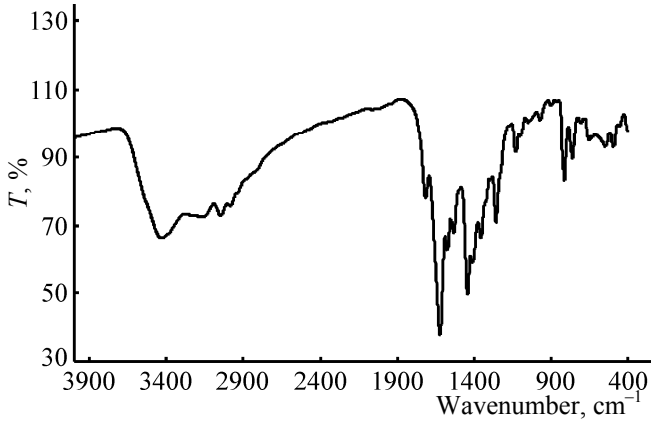

Fig. 4. IR spectrum of Ca(II) complex **I**.

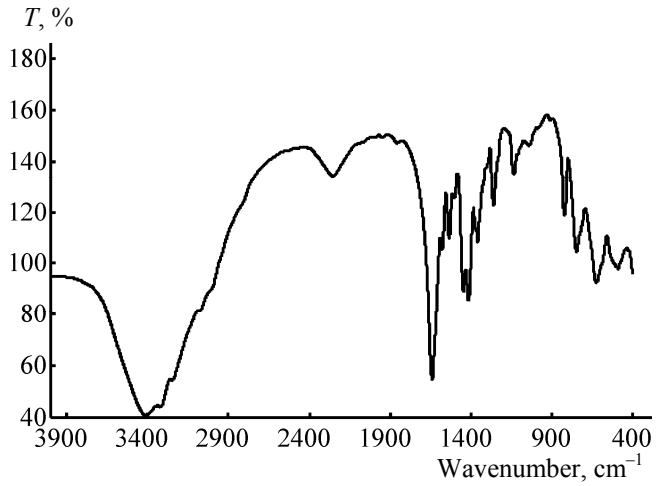

Fig. 5. IR spectrum of Mg(II) complex **II**.

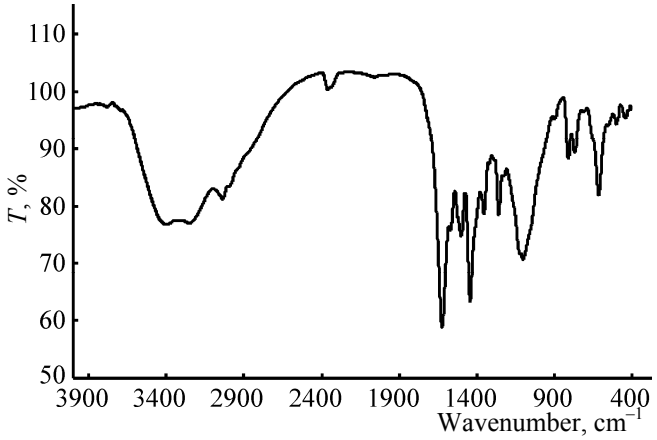

Fig. 6. IR spectrum of Zn(II) complex **III**.

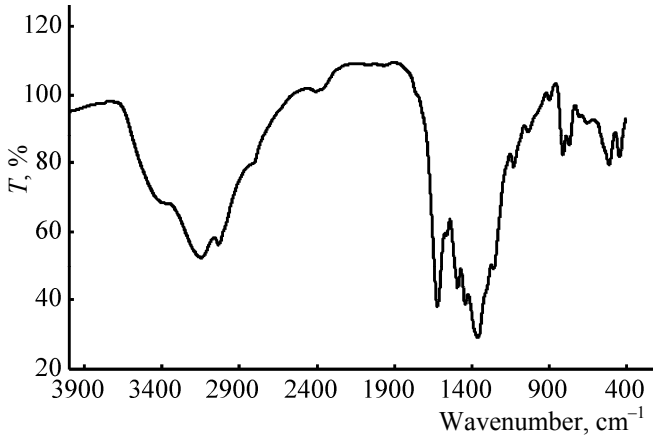

Fig. 7. IR spectrum of Fe(III) complex **IV**.

Table 3. [1]H NMR data of Nalidixic acid and its complexes

Compound	δ, ppm of hydrogen							
	H; –CH$_3$ (g)	H; –CH$_3$ (f)	H; OH$_2$	H; –CH$_2$- (e)	H; –CH (d)	H; –CH (c)	H; –CH (b)	H; –COOH (a)
Nalidixic acid	1.42	2.71	–	4.65	7.61	8.62	9.16	14.9
Ca(II) complex	1.37	2.66	3.30–3.39	4.57	7.49	8.52	9.07	–
Mg(II) complex	1.40	2.68	3.31–3.44	4.63	7.53	8.59	9.10	–

shows a broad band observed at 4310 cm^{-1}. This band can be assigned to the ν(OH) stretching vibration of OH in the COOH group. The infrared spectra of nalidixic acid complexes reveal a broad bands observed at 3400–3462 cm^{-1}. These bands can be assigned to the ν(OH) stretching vibration of the coordinated H_2O molecules. The IR spectral data of free nalidixic acid shows two very strong absorption peaks with high intensity at 1717 cm^{-1} due to ν(C=O) stretching vibration of the carboxylic group and at 1618 cm^{-1} which attributed to the ν(C=O) of the keto group in pyridine ring [39]. The Mg(II), Zn(II), Fe(III) and VO(II) complexes show no absorption band at 1717 cm^{-1} ν(C=O), except Ca(II) complex which shows very weak peak at 1715 cm^{-1} with very low intensity, that is indicative of the deprotonation of COOH group and involvement of the carboxyl group in the formation of M-O bonds. The ν(C=O) peak of keto pyridine ring is shifted from 1618 cm^{-1} up to 1620–1640 cm^{-1} upon binding [40]. The spectra of the complexes show two characteristic bands at 1573–1353, 1577–1358, 1570–1353, 1564–1360, and 1562–1360 cm^{-1} for Ca(II), Mg(II), Zn(II), Fe(III), and VO(II) complexes respectively, assigned as ν(COO$^-$) asymmetric and symmetric stretching vibrations of the chelated carboxylate anion respectively.

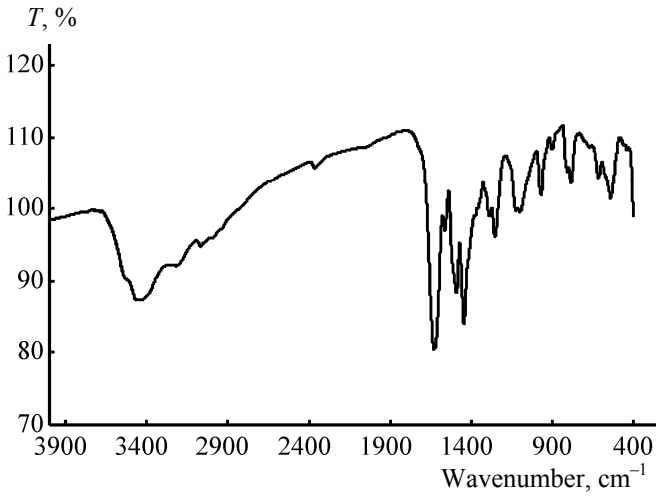

Fig. 8. IR spectrum of VO(II) complex **V**.

Deacon and Phillips, 1980 [41], have studied the criteria that can be used to distinguish between the three binding states of the carboxylate complexes. These criteria are: (a) Δν > 200 cm^{-1} (where Δν = [ν_{as}(COO$^-$) – ν_s(COO$^-$)]) this relation was found in case of monodentate carboxylate complexes, (b) bidentate or chelating carboxylate complexes exhibit Δν significantly smaller than ionic values (Δν < 100 cm^{-1}), and finally, (c) bridging complexes show Δν comparable to ionic values (Δν ~ 150 cm^{-1}). Therefore, the difference value Δν is a useful characteristic for determining the coordination mode of the carboxylate group of the ligands. The observed Δν Ca(II), Mg(II), Zn(II), Fe(III), and VO(II) complexes (Table 2) fall in the range 202–262 cm^{-1} indicating a monodentate coordination mode of the carboxylate group [42, 43]. The nalidixic acid complexes show a new bands observed at the range of 3145–3240 cm^{-1} which can be assigned to the stretching vibration of ν(N–H) of NH_3 and NH_4 groups, the absence of these bands in the spectrum of the free ligand support our explanation. Also the bending motions of δ(NH) observed at the range of 1441–1445 cm^{-1}. The ν(V=O) stretching vibration in the vanadyl complex **V** is observed as expected band at 968 cm^{-1}, which is in a good agreement with those known for many vanadyl complexes [44]. The coordination of NO_2 anion to the Fe(III) ions were also supported by the IR spectrum of the Fe(III) complex, that displayed three bands due to $\nu_{as}(NO_2)$ at 1564 cm^{-1}, $\nu_s(NO_2)$ at 1258 cm^{-1} and ν (NO) at 896 cm^{-1} assigned to monodentate group [45]. It is worth mentioned that the test for the presence of sulfate anions in the VO(II) and Zn(II) complexes gave a positive result. This conclusion was supported by observing two bands at about 1100 and 600 cm^{-1} overlapping with angular deformation motions of the coordinated water molecules. Participation of both carboxylate group and carbonyl group is also confirmed

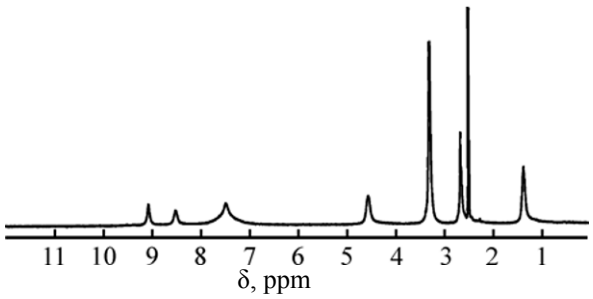

Fig. 9. [1]H NMR spectrum of Ca(II) complex **I**.

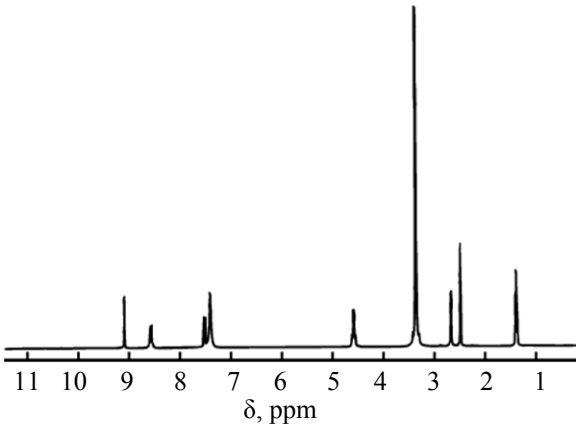

Fig. 10. [1]H NMR spectrum of Mg(II) complex **II.**

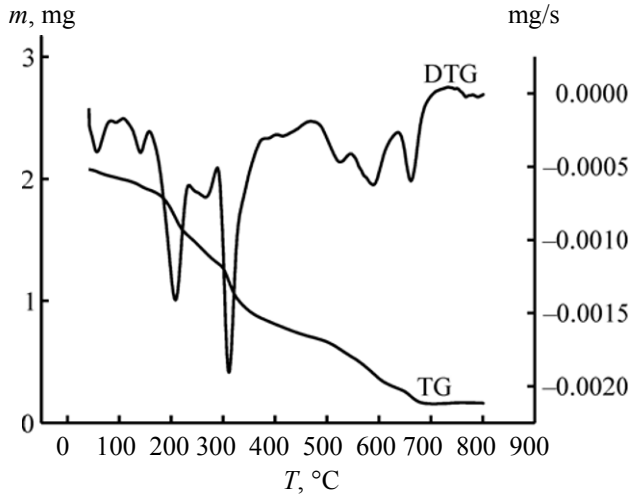

Fig. 11. TG/DTG curves of Ca(II) complex **I**.

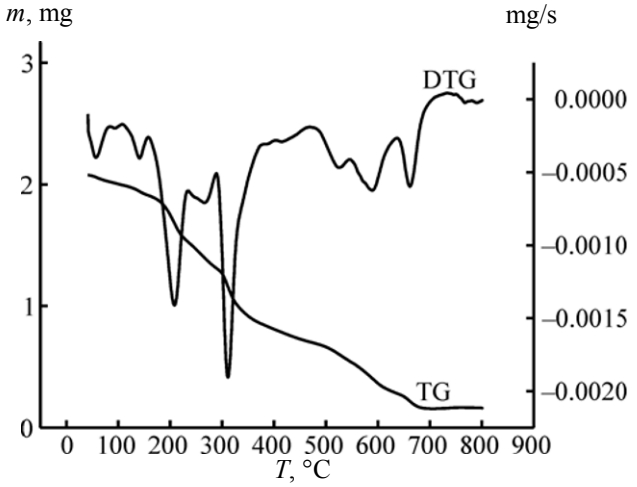

Fig. 12. TG/DTG curves of Mg(II) complex **II**.

by the appearance of new bands in the complexes at 500–622 and 438–487cm^{-1} regions which may be assigned to the ν(M–O) and ν(M–N) stretching vibration respectively [46, 47]. According to the IR data, the nalidixic acid is coordinated to the metal ions as bidentate ligand via one carboxylate oxygen atom and the oxygen atom of the pyridine ring carbonyl group [48].

^{1}H NMR studies. The ^{1}H NMR data of free nalidixic acid and its Ca(II) and Mg(II) complexes, as examples, are listed in Table 3 and shown in Figs. 9–10 [for Ca(II) complex **I** and Mg(II) complex **II**]. Upon comparison with the free ligand, the disappearance of the characteristic peak for hydrogen of –COOH at δ = 14.9 ppm in Ca(II) and Mg(II) complexes indicates that the coordination of nalidixic acid ligand to Ca(II) and Mg(II) occur through the deprotonated carboxylic group [38]. ^{1}H NMR spectra for Ca(II) and Mg(II) complexes show peaks at the range of 3.30–3.44 ppm, these peaks are not observed in the free ligand spectrum and can be assigned to the protons of H_2O molecules, supporting the complex formula. The overall changes of the ^{1}H NMR spectra of the Ca(II) and Mg(II) complexes are indicative of coordination of nalidixic acid ligand to the metal via the pyridone and one carboxylate oxygen atoms [49]. This suggested coordination is in agreement with that obtained by elemental analysis and IR spectra.

Thermal analysis. The obtained nalidixic acid complexes were studied by means of thermogravimetric (TG) and differential thermogravimetric (DTG/DTA) analysis in the range up to 800°C under nutrogen atmosphere. The TG curves were redrawn as mg mass loss versus temperature and DTG curves were redrawn as rate of loss of mass versus temperature. The thermal decomposition curves are given in Figs. 11–16 (TG/DTG curves) and Figs. 17–20 (DTA curves). Thermoanalytical results are summarized in Table 4.

Table 4. Thermal data

Compound	Steps	TG, °C	DTG_{max}, °C	DTA (°C)	TG weight loss, %		Assignments
					calculated	found	
I	1	39–232	57, 141 and 208	204 (*endo*)	22.53	23.32	$2H_2O+C_2H_4+NH_3$
	2	290–694	311, 525, 589 and 661	456 (*endo*)	66.34	66.69	$1/2Cl_2+C_{10}H_7N_2O_3$ (organic moiety)
	Final residue = Ca (found 10.01%, calculated 11.12%)						
II	1	25–70	42	–	3.83	3.53	$1.5H_2O$
	2	70–145	114	116 (*endo*)	14.07	14.05	$5.5H_2O$
	3	145–206	167	169 (*endo*)	8.96	9.06	$3.5H_2O$
	4	206–301	255	256 (*endo*)	14.07	14.39	$5.5H_2O$
	5	301–371	349	339 (*endo*)	5.11	4.72	$2H_2O$
	6	475–514	493	569 (*exo*)	10.23	10.28	$4H_2O$
	7	516–661	601	604 (*exo*)	22.67	22.21	$1/2Cl_2+NH_3+C_3H_{11}N_2O_2$ (organic moiety)
	Final residue = MgO + 9C (found 21.76% , calculated 21.03%)						
III	1	39–116	75	77 (*endo*)	7.46	7.05	$2H_2O$
	2	140–204	177	–	3.73	4.08	H_2O
	3	204–310	278	240 (*endo*)	24.04	23.14	$H_2O+H_2SO_4$
	4	310–387	337	355 (*endo*)	17.82	18.44	C_4H_8NO (organic moiety)
	5	511–677	568	566 (*exo*)	17.20	17.09	$C_3H_3N_2O$ (organic moiety)
	6	677–795	765	–	5.38	4.98	C_2H_2
	Final residue = ZnO + 3C (found 25.22%, calculated 24.33%)						
IV	1	40–119	72	–	3.74	2.75	H_2O
	2	119–286	216	–	40.33	41.01	$H_2O+2NH_4NO_3+CH_4$
	3	286–380	346	351 (*exo*)	16.63	16.35	C_4H_2NO (organic moiety)
	4	380–464	432	435 (*exo*)	21.83	23.30	C_6H_3NO (organic moiety)
	Final residue = FeO + C (found 16.59%, calculated 17.46%)						
V	1	67–177	115	96 (*endo*)	6.02	6.69	$1.5H_2O$
	2	177–320	268	261 (*endo*)	24.33	24.93	$0.5H_2O+H_2+H_2SO_4$
	3	320–455	407	416 (*exo*)	24.78	24.98	$NH_3+C_5H_4NO$ (organic moiety)
	4	455–529	485	489 (*exo*)	28.12	27.12	$C_5H_4NO_3$ (organic moiety)
	Final residue = V + 2C (found 16.58%, calculated 16.74%)						

Kinetic studies. Herein, the thermal behavior of the nalidixic acid complexes in terms of stability ranges, peak temperatures and values of kinetic parameters, are summarized in Table 5. Figures 21 and 22 show Coats-Redfern (CR) and Horowitz–Metzger (HM) plots of the first, second, third and fourth thermal decomposition steps of Ca complex **I**. From the kinetic and thermodynamic data resulted from the TGA curves and tabulated in Table 5, the following conclusions can be formulated:

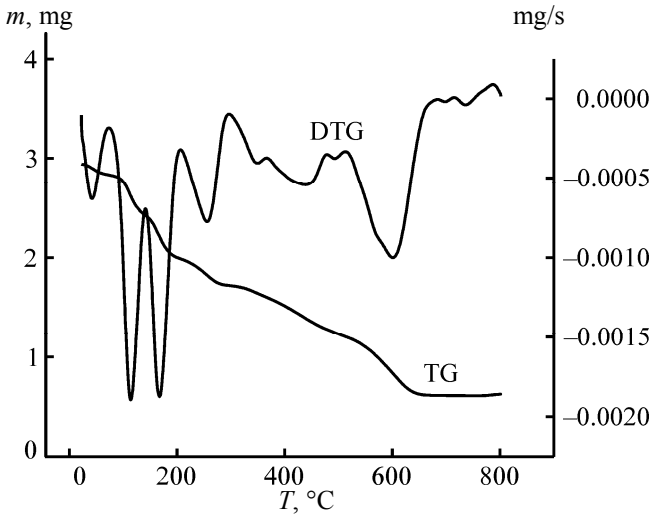

Fig. 13. TG/DTG curves of Zn(II) complex **III**.

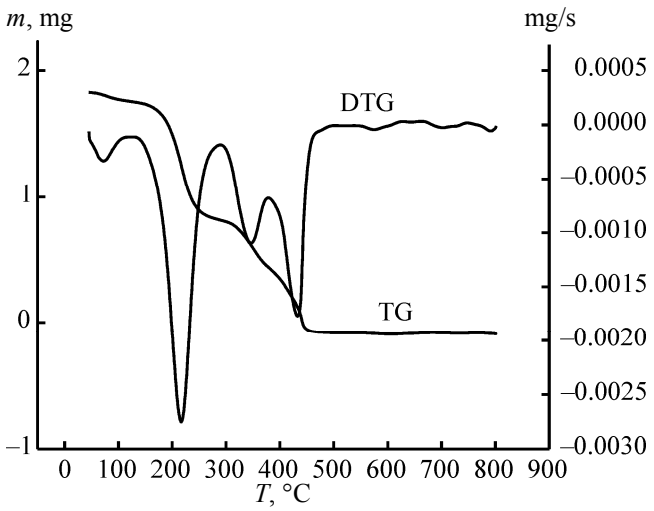

Fig. 14. TG/DTG curves of Fe(III) complex **IV**.

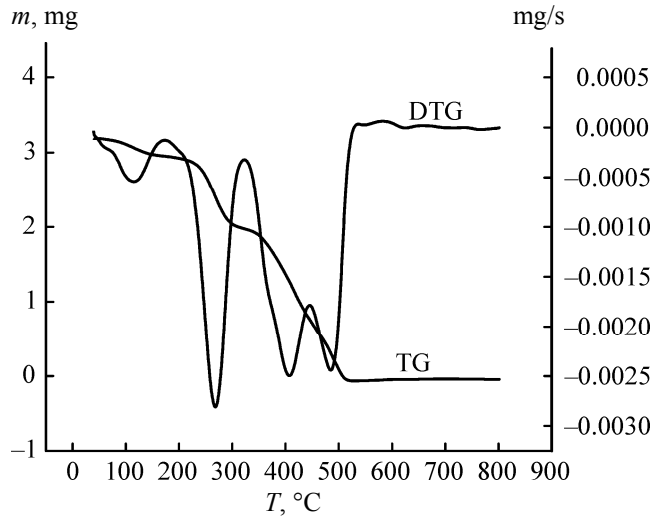

Fig. 15. TG/DTG curves of VO(II) complex **V**.

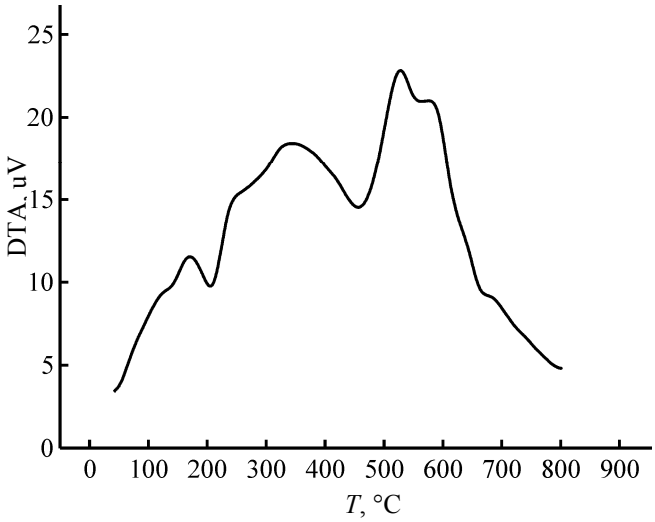

Fig. 16. DTA curve of Ca(II) complex **I**.

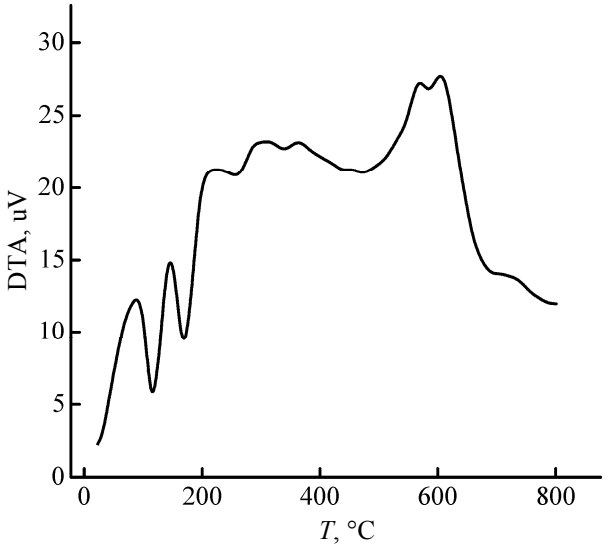

Fig. 17. DTA curve of Mg(II) complex **II**.

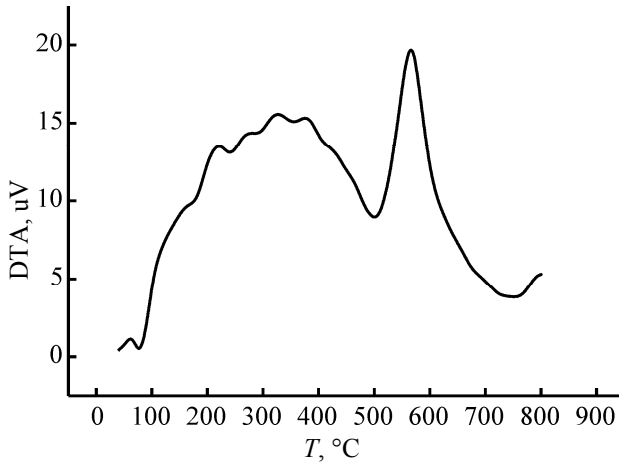

Fig. 18. DTA curve of Zn(II) complex **III**.

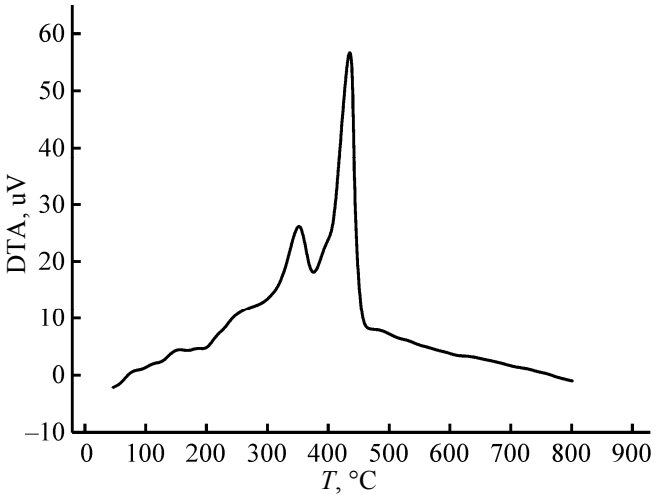

Fig. 19. DTA curve of Fe(III) complex **IV**.

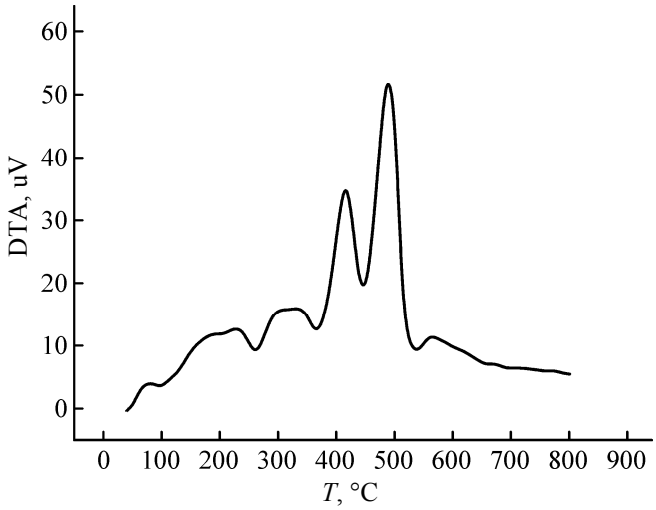

Fig. 20. DTA curve of VO(II) complex **V.**

(1) The higher values of activation energies of the nalidixic acid complexes led to thermal stability of the studied complexes.

(2) The thermodynamic data obtained with the two methods are in harmony with each other. The correlation coefficients of the Arrhenius plots of the thermal decomposition steps were found to lie in the range 0.9525–0.9998, showing a good fit with linear function.

(3) It is clear that the process of thermal decomposition of most nalidixic acid complexes is non-spontaneous (ΔS^* = negative value), i.e., the complexes are thermally stable.

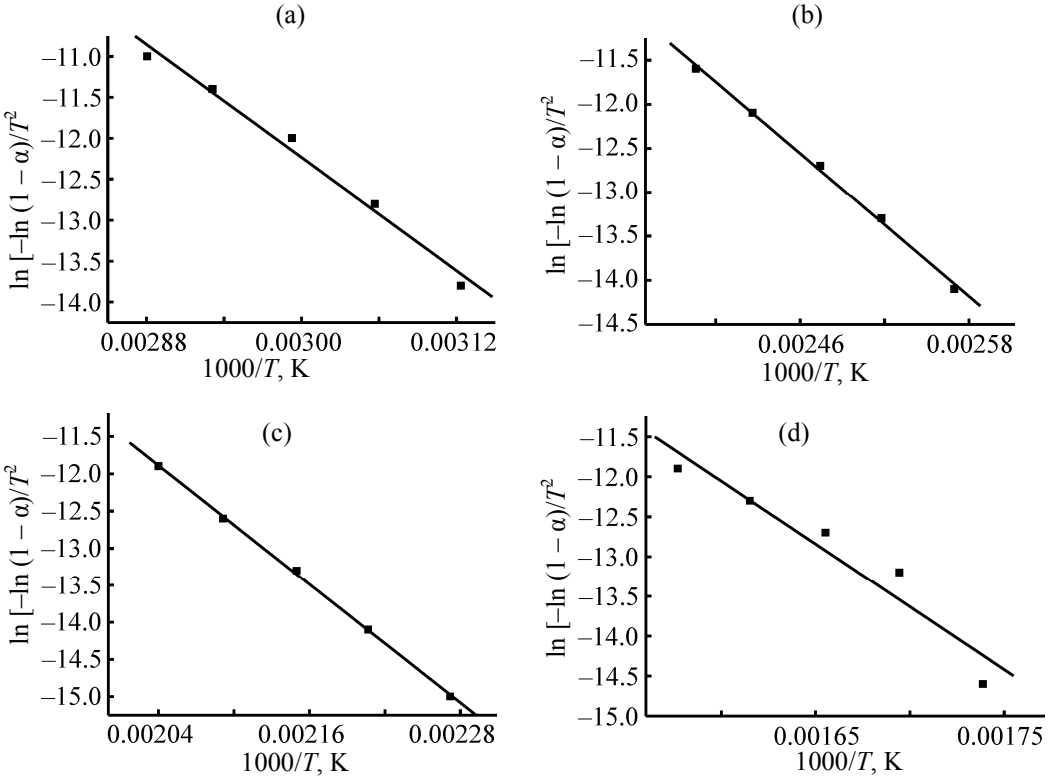

Fig. 21. Coats–Redfern (CR) plots of the (a) first, (b) second, (c) third, and (d) fourth thermal decomposition steps of Ca(II) complex **I**.

Table 5. Kinetic and thermodynamic parameters of the thermal decomposition of nalidixic acid complexes

Complex	Stage	Method	Parameter					Correlation coefficient r
			E, J mol^{-1}	A, s^{-1}	ΔS, J mol^{-1} K^{-1}	ΔH, J mol^{-1}	ΔG, J mol^{-1}	
I	1	CR	9.57E+04	1.41E+13	5.98E+00	9.30E+04	9.10E+04	0.99281
		HM	9.87E+04	1.24E+14	2.41E+01	9.59E+04	8.80E+04	0.99023
	2	CR	1.12E+05	3.26E+12	–8.10E+00	1.09E+05	1.12E+05	0.99872
		HM	1.24E+05	8.21E+13	1.87E+01	1.20E+05	1.12E+05	0.99777
	3	CR	1.11E+05	1.41E+10	–5.46E+01	1.07E+05	1.33E+05	0.99966
		HM	1.28E+05	1.44E+12	–1.61E+01	1.24E+05	1.32E+05	0.99872
	4	CR	1.31E+05	2.02E+09	–7.24E+01	1.26E+05	1.68E+05	0.96009
		HM	1.31E+05	6.32E+09	–6.29E+01	1.26E+05	1.63E+05	0.95251
II	1	CR	7.25E+04	8.74E+09	–5.51E+01	6.98E+04	8.72E+04	0.98363
		HM	7.34E+04	3.19E+10	–4.43E+01	7.07E+04	8.47E+04	0.97987
	2	CR	1.02E+05	6.78E+11	–2.06E+01	9.86E+04	1.07E+05	0.99663
		HM	1.12E+05	3.32E+13	1.18E+01	1.09E+05	1.05E+05	0.99436
	3	CR	1.13E+05	2.31E+11	–3.06E+01	1.09E+05	1.23E+05	0.97969
		HM	1.19E+05	2.21E+12	–1.18E+01	1.15E+05	1.20E+05	0.97836
	4	CR	1.06E+05	2.86E+08	–8.78E+01	1.01E+05	1.48E+05	0.99984
		HM	1.17E+05	5.04E+09	–6.39E+01	1.13E+05	1.47E+05	0.99711
III	1	CR	7.34E+04	9.15E+08	–7.47E+01	7.05E+04	9.65E+04	0.98859
		HM	7.92E+04	1.52E+10	–5.13E+01	7.63E+04	9.42E+04	0.98465
	2	CR	1.30E+05	1.73E+13	5.11E+00	1.26E+05	1.24E+05	0.99579
		HM	1.42E+05	5.89E+14	3.44E+01	1.38E+05	1.23E+05	0.99394
	3	CR	1.10E+05	2.61E+08	–8.89E+01	1.05E+05	1.54E+05	0.99441
		HM	1.30E+05	2.45E+10	–5.11E+01	1.25E+05	1.53E+05	0.99059
	4	CR	1.63E+05	6.58E+11	–2.46E+01	1.58E+05	1.73E+05	0.98666
		HM	1.70E+05	5.07E+12	–7.64E+00	1.65E+05	1.70E+05	0.98622
IV	1	CR	7.05E+04	2.82E+08	–8.44E+01	6.76E+04	9.68E+04	0.99201
		HM	7.50E+04	4.21E+09	–6.19E+01	7.21E+04	9.35E+04	0.98859
	2	CR	7.99E+04	2.00E+06	–1.28E+02	7.58E+04	1.39E+05	0.99531
		HM	3.41E+04	1.89E+01	–2.25E+02	3.01E+04	1.40E+05	0.98838
	3	CR	1.71E+05	2.63E+12	–1.32E+01	1.66E+05	1.74E+05	0.99564
		HM	1.91E+05	2.03E+14	2.29E+01	1.86E+05	1.72E+05	0.99518
	4	CR	2.09E+05	4.69E+13	9.65E+00	2.03E+05	1.97E+05	0.99216
		HM	2.28E+05	1.15E+15	3.62E+01	2.23E+05	1.97E+05	0.99546
V	1	CR	5.17E+04	5.33E+04	-1.57E+02	4.85E+04	1.09E+05	0.99053
		HM	5.65E+04	4.59E+05	-1.39E+02	5.33E+04	1.07E+05	0.98557
	2	CR	1.18E+05	1.74E+09	-7.30E+01	1.13E+05	1.53E+05	0.9916
		HM	1.28E+05	3.31E+10	-4.85E+01	1.24E+05	1.50E+05	0.98936
	3	CR	1.43E+05	8.74E+08	-8.06E+01	1.38E+05	1.93E+05	0.98956
		HM	1.64E+05	4.59E+10	-4.77E+01	1.59E+05	1.91E+05	0.9874
	4	CR	2.36E+05	2.00E+14	2.11E+01	2.30E+05	2.14E+05	0.99931
		HM	2.49E+05	2.06E+15	4.05E+01	2.43E+05	2.12E+05	0.99963

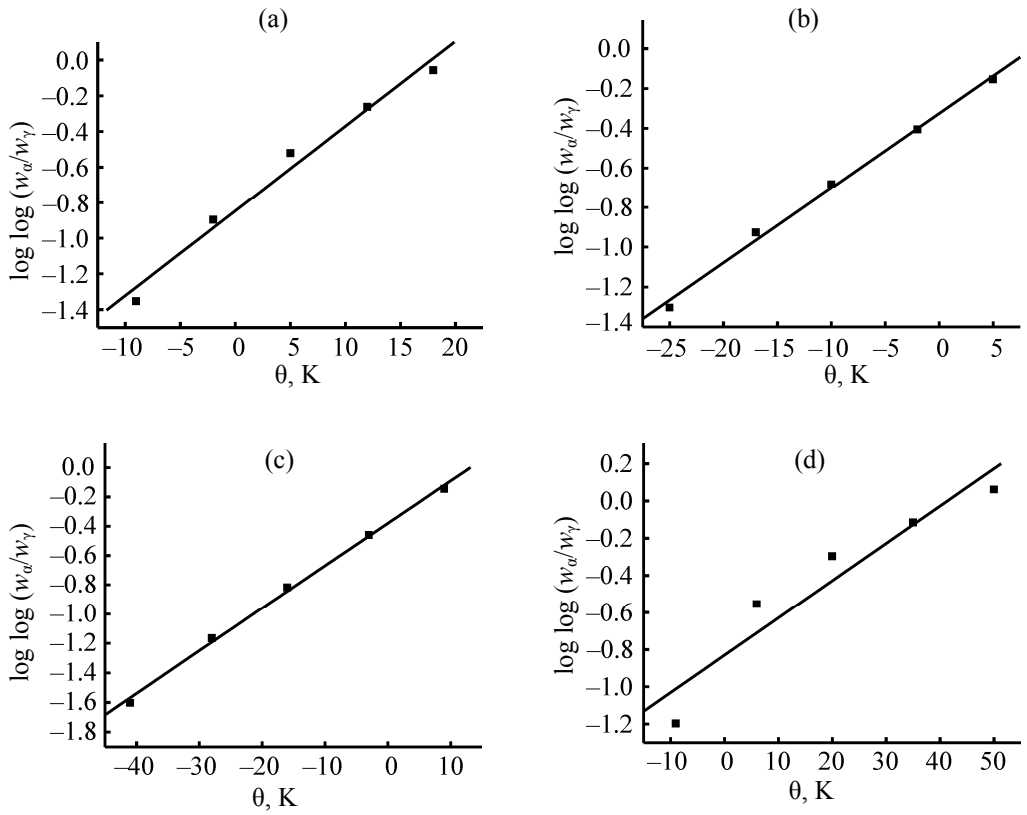

Fig. 22. Horowitz–Metzger (HM) plots of the (a) first, (b) second, (c) third, and (d) fourth thermal decomposition steps of Ca(II) complex **I**.

The thermograms and the calculated thermal parameters for the complexes show that the stability of these complexes depends on the nature of the central metal ion. The thermal stability of the metal complexes was found to increase periodically with increase in atomic number of the metal and the larger value of charge/radius ratio [50].

Structure of the nalidixic acid complexes. As a general conclusion, the structures of the investigated complexes can be given as shown in Figs. 23–27.

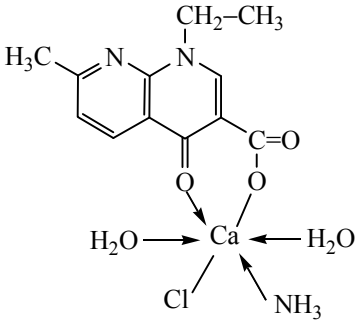

Fig. 23. Suggested structure of Ca complex of **I**.

Microbiological investigation of nalidixic acid complexes. *Microbiological investigation.* The hole well method according to Gupta et al. [34] was applied. The investigated isolates of bacteria and fungi were seeded in tubes with nutrient broth (NB) and Dox's broth (DB), respectively. The seeded (NB) for bacteria and (DB) for fungi (1 mL) were homogenized in the tubes with 9 mL of melted (45°C) nutrient agar (NA) for bacteria and (DA) for fungi. The homogenous suspensions were poured into Petri dishes. The holes (diameter 0.5 cm) were done in the cool medium.

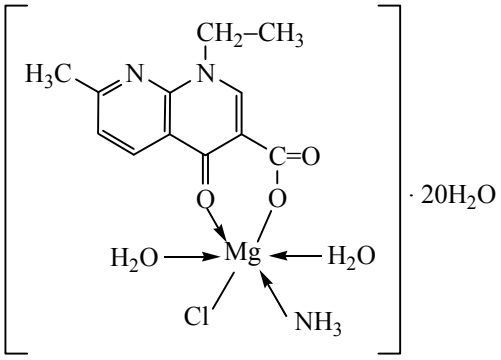

Fig. 24. Suggested structure of Mg complex **II**.

After cooling, in these holes, about 100 μL of the investigated compound solutions(concentration of each solution was 1.0×10^{-3} mol/L, commercial DMSO was used as a solvent) was applied using a micropipette. After incubation for 24 h in an incubator at 37°C and 28°C for bacteria and fungi, respectively, the inhibition zone diameter were measured and expressed in cm. The antimicrobial activities of the investigated compounds were tested against some kinds of bacteria such as *Escherichia coli* (Gramnegative) and *Staph albus* (Grampositive) as well as some kinds of fungi, such as *Aspergillus flavus* and *Aspergillus niger*. In the same time with the antimicrobial investigations of the complexes, the pure solvent also was tested as a blank. The free nalidixic acid was found to have the lowest activity against four types of bacteria and fungi, while the Zn(II) complex was found to have the highest activity. The biological activities increase in the following order: Zn(II)-Ndx > VO(II)-Ndx > Fe(III)-Ndx > Mg(II)-Ndx > Ca(II)-Ndx. The graphical representation of the data obtained is shown in Fig. 28.

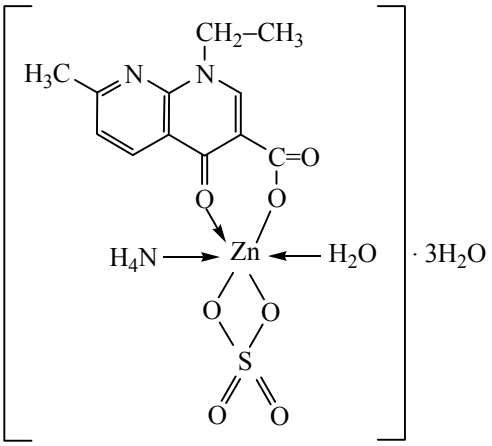

Fig. 25. Suggested structure of Zn(II) complex **III**.

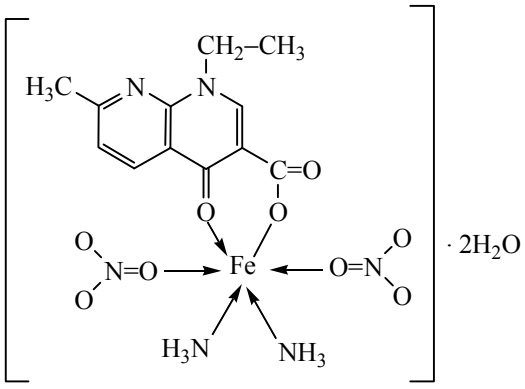

Fig. 26. Suggested structure of Fe(III) complex **IV.**

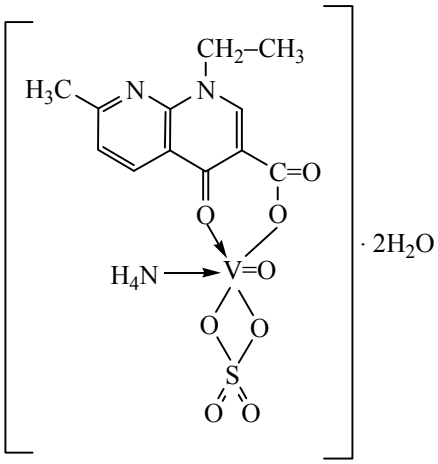

Fig. 27. Suggested structure of VO(II) complex **V**.

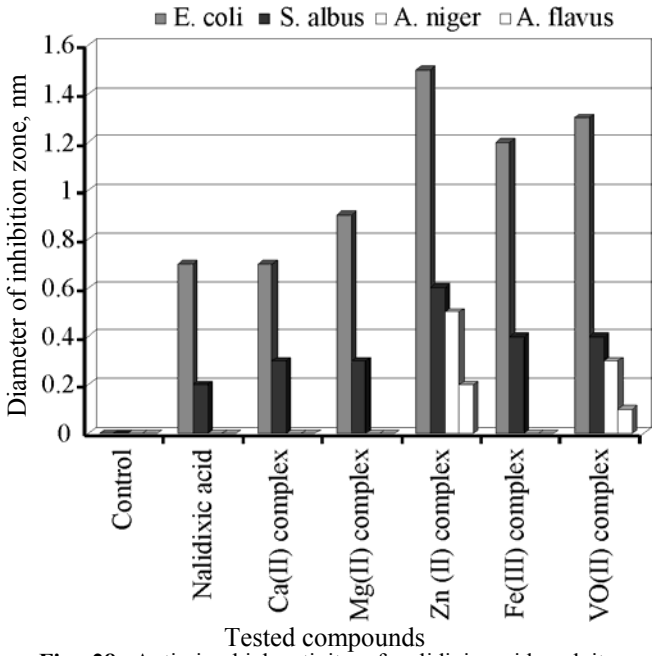

Fig. 28. Antimicrobial activity of nalidixic acid and its complexes.

REFERENCES

1. Albert, A., *The Physico-Chemical Basis of Therapy: Selective Toxicity*, London: Chapman & Hall, 1979, 6 ed.
2. *The Inorganic Chemistry of Biological Processes*, Hughes, M.N., Ed., New York: Wiley, 1981, 2 ed.
3. Liu, J., Wang, E.B., Peng, J., and Zhou, Y.S., *J. Rare Earths*, 1999, vol. 17, p. 139.
4. Chakrabarti, S., Dasgupta, D., and Bhattacharyya, D., *J. Biol. Phys.*, 2000, vol. 26, p. 203.
5. Smita, S., Anand, G., Ranjit, S., and Vikrant, V., *International Journal of Pharmaceutical Research and Development*, 2011, vol. 3, pp. 164–171.
6. Shaikh, A.R., Giridhar, R., and Yadav, M.R., *Int. J. Pharm.*, 2007, vol. 332, pp. 24–30.
7. Turel, I., *Coord. Chem. Rev.*, 2002, vol. 232, pp. 27–47.
8. Psomas, G., Tarushi, A., Efthimiadou, E.K., Raptopoulou, C.P., and Katsaros, N., *J. Inorg. Biochem.*, 2006, vol. 100, pp. 1764–1773.
9. Efthimiadou, E.K., Thomadaki, H., Sanakis, Y., Raptopoulou, C.P., Katsaros, N., Scorilas, A., and Pronas, G., *J. Inorg. Biochem.*, 2007, vol. 101, pp. 64–73.
10. Efthimiadou, E.K., Karaliota, A., and Psomas, G., *Polyhedron*, 2008, vol. 27, pp. 1729–1738.
11. Kumar Ajay and Danveer Singh Yadav, *Int. J. Chem. Sci*., 2009, vol. 7, no. 1, p. 19.
12. Skyrianou, K.C., Psycharis, V., Raptopoulou, C.P., Kessissoglou, D.P., and Psomas, G., *J. Inorg. Biochem.*, 2011, vol. 105, pp. 63–74.
13. Adam Abdel Majid, A., *J. Mater. Sci. Res.*, 2012, vol. 1, pp. 1–7.
14. Živec, P., Perdih, F., Iztok Turel, Giester, G., and Psomas, G., *J. Inorg. Biochem.*, 2012, vol. 117, pp. 35–47.
15. Zampakou, M., Akrivou, M., Andreadou, E.G., Raptopoulou, C.P., Psycharis, V., Pantazaki, A.A., and Psomas, G., *J. Inorg. Biochem.*, 2013, vol. 121, pp. 88–99.
16. Patel Mohan N., Chintan R. Patel, and Hardik N. Joshi, *Inorg. Chem. Commun.*, 2013, vol. 27, pp. 51–55.
17. King, D.E., Malone, R., and Lilley, S.H., *Am. Fam. Physician*, 2000, vol. 61, pp. 2741–2748,
18. *The Quinolones*, Andriole, V.T., Ed., San Diego: Academic Press, 2000, 3 ed.
19. Lesher, G.Y., and Gruett, M.D., Belgian Patent no. 612.258, 1962.
20. Ruzicka, E., Lasovsky, J., and Brazdil, P., *Chem. Zvesti*, 1975, vol. 29, p. 517.
21. Timmers, K. and Sternglanz, R., *Bioinorg. Chem.*, 1978, vol. 9, p. 145.
22. Nakano, M., Yamamoto, M., and Arita, T., *Chem. Pharm. Bull.*, 1978, vol. 26, p. 1505.
23. Vicent, W.R., Schulman, S.G., Midgley, J.M., van Oort, W.J., and Sorel, R.H.A., *Int. J. Pharm.*, 1981, vol. 9, p. 191.
24. Panadero, S., Gómez-Hens, A., and Pérez-Bendito, D., *Anal. Chim. Acta*, 1995, vol. 303, p. 39.
25. Kljun, J., Bytzek, A.K., Kandioller, W., Bartel, C., Jakupec, M.A., Hartinger, C.G., Keppler, B.K., and Turel, I., *Organometallics*, 2011, vol. 30, p. 2506.
26. Freeman, E.S. and Carroll, B., *J. Phys. Chem*., 1958, vol. 62, p. 394.
27. Coats, A.W. and Redfern, J.P., *Nature*, 1964, vol. 201, p. 68.
28. Ozawa, T., *Bull. Chem. Soc. Jap*., 1965, vol. 38, p. 1881.
29. Wendlandt, W.W., *Thermal Methods of Analysis*, New York: Wiley, 1974.
30. Horowitz, H.W. and Metzger, G., *Anal. Chem*., 1963, vol. 35, p. 1464.
31. Flynn, J.H. and Wall, L.A., *Polym. Lett*., 1966, vol. 4, p. 323.
32. Kofstad, P., *Nature*, 1957, vol. 179, p. 1362.
33. Flynn, J.H.F. and Wall, L.A., *J. Res. Natl. Bur. Stand*., 1996, vol. 70A, p. 487.
34. Gupta, R., Saxena, R.K., Chatarvedi, P., and Virdi, J.S., *J. Appl. Bacteriol*., 1995, vol. 78, p. 378.
35. Refat, M.S., *J. Mol. Struct*., 2007, vol. 842, nos. 1–3, p. 24.
36. Vogel, T., *Textbook of Practical Organic Chemistry*. London: Wiley, 1989, 4 ed., p. 133.
37. Polishchuk, A.V., Karaseva, E.T., Emelina, T.B., Nikolenko, Y.M., and Karasev, V.E., *J. Stru. Chem*., 2009, vol. 50, no. 3, p. 434.
38. Refat, M.S., *Spectrochimica Acta Part A*, 2007, vol. 68, p. 1393.
39. Sadeek, S.A., El-Didamony, A.M., El-Shwiniy, W.H., and Zordok, W.A., *J. Argent. Chem. Soc*., 2009, vol. 97, p. 51.
40. Efthimiadou, E.K., Thomadaki, H., Sanakis, Y., Raptopoulou, C.P., Katsaros, N., Scorilas, A., and Pronas, G., *J. Inorg. Biochem.*, 2007, vol. 101, p. 64.
41. Deacon, G.B. and Phillips, R.J., *Coord. Chem. Rev*., 1980, vol. 33, p. 227.
42. Dendrinou-Samara, C., Tsotsou, G., Ekateriniadou, L.V., Kortsaris, A.H., Raptopoulou, C.P., Terzis, A.,

Kyriakidis, D.A., and Kessissoglou, D.P., *J. Inorg. Biochem*., 1998, vol. 71, p. 171.

43. Nakamoto, K., *Infrared and Ramman Spectra of Inorganic and Coordination Compounds*, New York: Wiley, 1986, 4 ed., p. 230.
44. Bhattacharyya, S., Mukhopadhyay, S., Samanta, S., Weakley, T.J.R., and Chaudhury, M., *Inorg. Chem*., 2002, vol. 41, p. 2433.
45. Mohamed, G.G., *Spectrochim. Acta Part (A)*, 2001, vol. 57, p. 1643.
46. Zayed, M.A., Nour El-Dien, F.A., Mohamed, G.G., and El-Gamel, N.E.A., *Spectrochim. Acta Part (A)*, 2004, vol. 60, p. 2843.
47. Santi, E., Torre, M.H., Kremer, E., Etcheverry, S.B., and Baran, E., *Vib. Spectrosc*., 1993, vol. 5, p. 285.
48. Turel, I., *Coord. Chem. Rev*., 2002, vol. 232, p. 27.
49. Riley, C.M., Ross, D.L., van der Velde, D., and Takusagawa, F., *J. Pharm. Biomed. Analysis*, 1993, vol. 11, p. 49.
50. Malik, W., Tuli, G.D., and Madan, R.D., *Selected Topics in Inorganic Chemistry*, New Delhi: Chand and Co. Ltd., 1984.